Published in final edited form as:
*Nat Cell Biol*. 2009 November ; 11(11): 1363–1369. doi:10.1038/ncb1983.

# UBE2S elongates ubiquitin chains on APC/C substrates to promote mitotic exit

**Mathew J. Garnett**[1,3], **Jörg Mansfeld**[2,3], **Colin Godwin**[1], **Takahiro Matsusaka**[2], **Jiahua Wu**[1], **Paul Russell**[1], **Jonathon Pines**[2], and **Ashok R. Venkitaraman**[1]

[1] University of Cambridge, Department of Oncology & The Medical Research Council Cancer Cell Unit, Hutchison/MRC Research Centre, Hills Road, Cambridge, CB2 OXZ, UK.

[2] Wellcome/CR UK Gurdon Institute and Department of Zoology, Tennis Court Road, Cambridge, CB2 1QN, UK

## Abstract

The anaphase-promoting complex (APC/C) ubiquitin ligase is the target of the spindle-assembly checkpoint (SAC), ubiquitylating protein substrates whose degradation regulates progress through mitosis1-3. The identity of the ubiquitin-conjugating (E2) enzymes that work with the APC/C is unclear. In an RNA interference screen for factors that modify release from drug-induced SAC activation, we identify here the E2 enzyme, UBE2S, as an auxillary factor for the APC/C that promotes mitotic exit. UBE2S is dispensable in a normal mitosis, but its depletion prolongs drug-induced mitotic arrest and suppresses mitotic slippage. *In vitro*, UBE2S elongates ubiquitin chains initiated by the E2 enzymes UBCH10 and UBCH5, enhancing the degradation of APC/C substrates by the proteasome. Indeed, following release from SAC arrest, UBE2S-depleted cells neither degrade crucial APC/C substrates, nor silence this checkpoint, whereas SAC bypass via BUBR1 depletion or Aurora-B inhibition negates the requirement for UBE2S. Thus, UBE2S acts with the APC/C in a two-step mechanism controlling substrate ubiquitylation that is essential for mitotic exit after prolonged SAC activation, providing a new model for APC/C function in human cells.

Inactivation of the SAC when all chromosomes receive a bi-polar attachment to spindle microtubules1 allows the APC/C to mark cell cycle regulated proteins such as Cyclin B1 and Securin for degradation by the 26S proteasome, thereby initiating anaphase4, 5. Which E2 enzyme(s) work with the APC/C *in vivo* is unclear: *in vitro*, the APC/C can work with the Ubc4/5 and E-2C families (in particular, human UBCH5 and UBCH10, respectively)6. Evidence from simple model organisms indicates that E2-C family members are most likely to be biologically relevant7-12, but siRNA studies in human cells disagree over whether UBCH10 is essential for mitosis13, 14. Moreover, APC/C activity in model organisms may not depend solely on a single E2 partner. For instance, budding yeast Ubc1 serves as a supplementary E2 enzyme that elongates ubiquitin chains initiated by a proximally-acting E211. This could be an important determinant of the efficiency of APC/C-targeted degradation, and thus exit from mitosis, because ubiquitin chain length modulates recognition by the proteasome15. The mechanism and efficiency of APC/C-targeted degradation likely affect the cellular outcomes of mitotic arrest induced by anti-cancer drugs

Correspondence should be addressed to M.J.G and A.R.V., arv22@cam.ac.uk.
[3]These authors contributed equally to this work

**AUTHOR CONTRIBUTIONS** M.J.G, A.R.V. and P.R. designed the siRNA screen; M.J.G. and C.G. performed the screen; M.J.G, C.G., P.R. and J.W. analyzed the screen data. M.J.G performed the analysis of UBE2S cellular function. J.M. performed the APC/C *in vitro* activity assays, and T.M., the Cyclin-B1 degradation assays and microinjection studies. M.J.G and T.M performed the time-lapse studies, which J.W. helped quantify. All authors analyzed and interpreted the data. The manuscript was written by M.J.G and A.R.V.


Europe PMC Funders Author Manuscripts

like taxanes, following which cells undergo mitotic slippage, and may either abnormally exit mitosis to form aneuploid progeny, or die16-18.

We have searched for genes that modify release from drug-induced mitotic arrest (Figure 1a) in human Cal51 cells. We used siRNA to deplete 520 components of the ubiquitin-proteasome system (Supplemental Information, Table 1), and determined the percentage of mitotic cells (mitotic index; MI) by high-content microscopy (Figure 1b). The MI of cells 20 hours after release from exposure to Monastrol (Mona, $MI_{Mona}$), was compared to DMSO-treated control cells ($MI_{DMSO}$). A difference value, $\Delta MI = MI_{Mona} - MI_{DMSO}$, was calculated for each siRNA (Figure 1c). The screen results are summarised in Supplemental Information, Table 2. Putative hits were defined to have a ΔMI standard score >2, and are significantly different from a non-targeting siRNA (p-value <0.01, Student's t-test). UBE2S (also known as E2-EPF) and PRPF8 were the only two candidates fulfilling these criteria. PRPF8 was not further studied because at later time-points its depletion induced mitotic arrest even without Mona (data not shown). The phenotypic effects of UBE2S depletion were confirmed using four different siRNA oligos targeting discrete regions of the transcript (Figure 1d), with the largest increase observed for oligo D2 (Figure 1e).

We compared the ΔMI in UBE2S-depleted cells whilst continually exposed to Mona, and 20 hours after release from exposure (Figure 2a and b). Only 35%-70% of UBE2S-depleted cells exited mitosis during this period compared with 90% of control cells. UBE2S depletion also suppressed mitotic slippage in cells continually exposed to Mona (Figure 2b). Only 25%-35% of UBE2S-depleted cells underwent mitotic slippage during continual drug exposure, versus ~60% of controls.

UBE2S depletion significantly impaired the ability to resume mitotic progression after exposure to S-trityl-l-cysteine and Dimethylenastron (which, like Mona, inhibit the mitotic kinesin Eg5 19-22), or mitotic inhibitors with different modes of action such as taxol and nocadazole, which respectively stabilize or suppress microtubule assembly (Figure 2c). UBE2S depletion had the largest effect after taxol exposure, and the smallest after Mona, consistent with the magnitude of the initial mitotic arrest induced by these compounds (see Figure 5c). These effects were manifest in several cell types, including the cervical cancer cell line, HeLa, as well as immortalized Retinal Pigmented Epithelial (RPE) cells (Figures 2d and e).

We examined more closely the kinetics of checkpoint arrest and mitotic slippage after UBE2S depletion, by analysing Mona-arrested cells released into drug-free media. Approximately 35% of control-treated cells exit mitosis in the first 3 hours, and the majority (85%) by 12 hours (Figure 3a). UBE2S depletion significantly delayed mitotic exit; even by 12 hours, only about 30% of cells had exited. A similar delay occurs in individual cells examined by time-lapse imaging (Figure 3b). The average time to exit mitosis after release from drug-induced arrest was 255 +/− 169 minutes ($n$=49 cells) in controls versus 668 +/− 412 minutes ($n$=48) after UBE2S depletion. Similar effects occurred after release from a short (6 hour) arrest in synchronised cells; thus, the duration of arrest did not alter the requirement for UBE2S (Supplemental Information, Fig. S1a).

UBE2S also influenced mitotic slippage during sustained inhibitor treatment (Figure 3c). In contrast to controls, UBE2S depletion markedly decreased mitotic slippage, with an increased MI 24 hours after taxol addition, and a delay in mitotic slippage by the majority of cells to some 72 hours after taxol addition. Moreover, by time-lapse imaging there was a significant increase in the duration of mitosis. Some 90% ($n$=87) of control cells undergo slippage within 1000 minutes (~17 hours), whereas during the same period, only 47% ($n$=109) of UBE2S-depleted cells do (Figure 3d).

A small increase in the MI occurs following UBE2S depletion even without any inhibitor (Figure 2b, oligo D2), prompting us to examine closely the role of UBE2S in normal mitosis using time-lapse microscopy with cell lines expressing Histone H2B-GFP. UBE2S depletion only modestly increased the time from nuclear envelope breakdown (NEBD) to anaphase in HeLa or Cal51 cells (Figure 3e), and did not detectably affect the degradation of Cyclin B1-GFP (Supplemental Information, Fig. S1b). In Cal51 cells, the average duration of mitosis significantly increased from 28.7 +/− 14 minutes ($n$=110 cells) in controls, to 34.1 +/− 14.4 minutes ($n$=113) after UBE2S depletion ($p<0.01$). In HeLa cells (Figure 3e), the average duration increased from 43.4 +/− 17.2 minutes ($n$=174 cells) in controls to 55 +/− 23 minutes after UBE2S depletion ($n$=124; $p<0.001$). In contrast, however, micro-injection of an untagged, catalytically-inactive form of UBE2S into HeLa cells did not lengthen mitosis (46.6 +/− 9.6 min; $n$=19) compared to injection with wild-type UBE2S (42 +/− 15 min; $n$=24 cells; $p>0.1$) or even uninjected cells (53.5 +/− 27.9 min; $n$=89). Thus, our findings indicate that UBE2S is largely dispensable in an unperturbed mitosis but may have a modest and non-essential function. Alternatively, although UBE2S depletion with RNAi eliminates any protein detectable by Western blotting, very small amounts may nevertheless persist, satisfying any requirement during a normal mitosis.

We determined the effect of UBE2S on the ubiquitylation of the anaphase inhibitors Cyclin B1 and Securin using a reconstituted *in vitro* APC/C activity assay with purified protein components. In these assays, the APC/C ubiquitylated an N-terminal fragment of Cyclin B1 (aa 1-86) when incubated with the E2 enzymes, UBCH10 or UBCH5 (Figure 4a). In contrast, incubation of UBE2S alone with the APC/C did not catalyse ubiquitylation of Cyclin B1 (Fig 4a) or Cyclin A (Supplemental Information, Fig. S2a) or Securin (data not shown). Notably, however, when UBE2S was added to the assays together with UBCH10 or UBCH5, the number of conjugated ubiquitin molecules per Cyclin B1 was significantly increased (Figure 4a). Since UBE2S did not catalyse substrate ubiquitylation on its own, this result indicated that UBE2S either enabled UBCH10 and UBCH5 to ubiquitylate additional lysines on Cyclin B1, or that it elongated ubiquitin chains on pre-ubiquitylated lysines. To distinguish between these possibilities, we used methylated ubiquitin, which prevents the elongation but not initiation of ubiquitin chains (Figure 4b). UBE2S did not affect UBCH10 or UBCH5 ubiquitylation of Cyclin B1 when using methylated ubiquitin, confirming that it can elongate ubiquitin chains on pre-ubiquitylated lysines, but does not initiate conjugation.

In budding yeast the E2 enzyme Ubc1 extends ubiquitin chains pre-attached by the APC/C11. Therefore we measured whether UBE2S could extend ubiquitin chains on a pre-ubiquitylated Cyclin B1 substrate. Unexpectedly, we could not detect this activity with UBE2S alone, whereas the human homologue of yeast Ubc1 (E2-25K) and UBCH10 extended ubiquitin chains under the same conditions (Supplemental Information, Fig. S2b). This result may indicate UBE2S elongates ubiquitin chains by a different mechanism from enzymes such as E2-25K.

When we quantified the proportion of Cyclin B1 conjugated with 1-4, 5-9 or >9 ubiquitin molecules (Figure 4c), we found both UBCH10 and UBCH5 primarily conjugated between 1 and 4 ubiquitin molecules to Cyclin B1, but the addition of UBE2S significantly increased the proportion of Cyclin B1 with >9 ubiquitin molecules (Figure 4c). Representative activity assays used for the quantification are provided in Supplemental Information, Figure S3. A catalytically inactive version (C95S) of UBE2S was unable to promote longer chains, and combining UBCH5 and UBCH10 did not drastically change the chain length compared to UBCH5 alone (Figure 4a and 4c). Similarly, combining UBCH10, UBCH5 and UBE2S together in a single ubiquitylation reaction did not increase polyubiquitination above reactions using UBE2S/UBCH10 or UBE2S/UBCH5 (Supplemental Information, Fig. S4).

The addition of UBE2S to UBCH10 reactions reduced total ubiquitylation at earlier time-points and this was dependent on UBE2S catalytic activity (Figure 4c, compare 10 minute time-points from UBCH10, UBCH10/UBE2S and UBCH10/UBE2S C95S). Possibly UBE2S and UBCH10 compete for binding to the APC/C; alternatively, substrates could dwell longer on a ternary APC/C-UBCH10-UBE2S complex, in keeping with the requirement for pre-ubiquitylation by another E2 to precede UBE2S activity.

Our cellular studies indicated that the action of UBE2S might become more important for efficient substrate degradation when APC/C activity had been compromised by a prolonged SAC arrest. To test this, drug-arrested cells were collected by mitotic shake-off, and samples taken 3 and 9 hours post-release for Western blotting of APC/C substrates. In control cells, Cyclin B1 and Securin protein levels were high during mitotic arrest and mostly degraded by 3 hours post-release (Figure 5a). In contrast, UBE2S depletion suppressed degradation of Cyclin B1 and Securin even at 9 hours post-release. Additionally, the early mitotic APC/C substrates Cyclin A and Nek2A23, 24, which are degraded during pro-metaphase when the SAC is active, accumulated in cells depleted of UBE2S (Figure 5a).

To quantify precisely the effect of UBE2S on substrate degradation, we measured levels of GFP-tagged Cyclin B1 during mitotic slippage (Figure 5b). As expected18, 25, we observed a slow decline in Cyclin B1 levels during arrest, and a rapid decline around 10 minutes before exit from mitosis. Since UBE2S-depleted cells exhibited a prolonged mitotic arrest, (Figure 3c and 3d), we measured the levels of Cyclin B1 specifically during the slow degradation stage (Figure 5b). Compared with controls, in cells depleted of UBE2S the rate of Cyclin B1 degradation decreased (from a slope of $-1.4 \times 10^{-3}$ to $-0.65 \times 10^{-3}$ fluorescence units per minute) and the duration of mitotic slippage was significantly extended. In contrast, UBE2S depletion had little effect on Cyclin B1 degradation during a normal unperturbed mitosis (Supplemental Information, Fig. S1b), suggesting that it only becomes rate-limiting after drug-induced SAC activation. Indeed, we find that mitotic arrest was evident in both control and UBE2S-depleted cells treated for 20 hours (t=20 arrest) with 12.5 μM Mona, but not with lower doses (Figure 5c). Correspondingly, UBE2S became necessary for mitotic exit after release from mitotic arrest (t=40 release) and for slippage (t=40 constant) only at ~12.5 μM Mona. Similar results were obtained when cells were treated with a range of taxol concentrations (data not shown).

Interestingly, BUBR1 protein levels were increased in arrested cells depleted of UBE2S, and BUBR1 was hyper-phosphorylated, indicating that the SAC was active (Figures 5a and 5d). BUBR1 forms an inhibitory complex with the APC/C co-activator CDC201, 3, whose presence is a measure of SAC activity. In control cells, BUBR1 was complexed with CDC20 at the time of arrest (t=0), and the CDC20-BUBR1 interaction was lost 9 hours after release during mitotic exit (Figure 5d). Following UBE2S depletion, however, BUBR1-CDC20 complex formation was increased both at the time of arrest, and 9 hours following release, despite lower levels of CDC20 and BUBR1, indicating that the SAC remained active at least in a proportion of UBE2S-depleted cells.

A BUBR1 mutant resistant to APC/C-mediated degradation delays anaphase entry26. However, we find that both endogenous BUBR1, which co-purifies with the APC/C from SAC arrested HeLa cells27, and recombinant BUBR1 are poor APC/C substrates *in vitro* (Supplemental Information, Fig. S5). Therefore, although UBE2S may contribute to SAC inactivation by enhancing APC/C-mediated ubiquitylation of BUBR1, under our *in vitro* conditions BUBR1 is not a preferred substrate, and so other substrates may be involved *in vivo*.

If UBE2S helps to inactivate the SAC, then forced SAC inactivation should bypass the requirement for UBE2S in exit from mitosis. Indeed, co-depleting UBE2S with BUBR1 prevented mitotic arrest following treatment with Mona or taxol (Figure 5e). Strikingly, the Aurora kinase inhibitor ZM 44743928, which acutely inactivates the SAC in arrested cells (Figure 5f and 5g), triggered mitotic exit within 3 hours in both control and UBE2S-depleted cells (Figure 5f), whereas cells depleted of the APC/C co-activator CDC20 failed to exit mitosis even after 6 hours. Moreover, Cyclin B1 was degraded following ZM 447439 exposure in control and UBE2S-depleted cells (Figure 5g), consistent with its efficient APC/C-mediated degradation even after UBE2S depletion. Thus collectively, our data indicate that UBE2S is necessary and rate-limiting for SAC inactivation following drug-induced mitotic arrest.

In contrast, UBE2S depletion has little effect on normal mitotic progression (Figure 3e), and is largely dispensable for Cyclin B1 degradation in this setting (Supplemental Information, Fig. S1b). We explain this difference as follows. The activity of the APC/C in ubiquitylating and promoting the proteasomal degradation of its substrates is normally opposed by the activity of antagonistic de-ubiquitylating enzymes29-31. UBE2S, by enhancing the formation of elongated ubiquitin chains, should shift the equilibrium between these opposing activities, favouring substrate degradation by facilitating proteasomal recognition15. Although UBE2S may also act during an unperturbed mitosis, its role becomes rate-limiting during release from drug-induced SAC activation. This role is apparently both general and essential, manifesting in several cell types exposed to different anti-mitotic drugs. In this setting, it appears that UBE2S is important to silence the SAC, since forced SAC inactivation suffices to bypass UBE2S depletion and allow mitotic progression. Thus, our findings identify UBE2S as an unrecognised regulator of mitosis, and suggest a new, two-step model for human APC/C function in which the E2 activity of UBE2S elongates ubiquitin chains initiated by a proximally-acting E2, to promote APC/C-targeted substrate degradation.

## METHODS

### siRNA library screening and high content microscopy

All steps were performed in 96-well plates using a BiomekNX$^{P}$ liquid-handling workstation (Beckman Coulter). A custom-made 535 oligo siRNA library targeting 520 components of the Ubiquitin-proteasome system was provided by Prof. Paul Lehner (University of Cambridge) and purchased from Dharmacon. siRNAs in the library target human E1, E2 and E3 ubiquitin-conjugating enzymes and de-ubiquitinating enzymes (Supplemental Table S1). Triplicate reverse transfections were performed in 96-well plates using Dharmafect I with 20,000 Cal51 cells and 25 nM on-target plus siRNA pools containing 4 siRNA targeting an individual gene (Dharmacon). 24 hours following transfection Monastrol (100 μM) or solvent control (DMSO) was added to triplicate plates for 20 hours. During this period cells arrest in mitosis and some cells begin to undergo mitotic slippage. Media was then aspirated from wells and replaced with fresh media before leaving for an additional 20 hours. The control samples were collected 20 hours following DMSO addition. Cells were fixed in 70% EtOH and stored at 4°C. For antibody staining cells were incubated in blocking solution (TBS, 0.1% Triton-X100 and 2% BSA) for 20 minutes, and then stained in blocking solution with the mitotic marker mouse anti-phospho S10 Histone H3 (pSer10-H3, 1:1,000 dilution, Abcam) for 1 hour at room temperature. Secondary antibody was conjugated with Alexa-633 dye (Invitrogen) and incubated for 1 hour at room temperature in blocking buffer. Following antibody staining, DNA was stained with 4 μg/ml Hoechst 33452 (Sigma) in PBS for 30 minutes. Plates were sealed and stored in PBS at 4°C in the dark prior to analysis.

Fluorescence images of stained cells were collected using a Cellomics Arrayscan high content fluorescence microscope (Thermo Scientific) and analysed using the Cellomics Morphology Explorer Bioapplication. DNA staining was used for object selection and data was collected for >5000 objects (cells) in each well (or 40 images) to generate a histogram of raw average pSer10-H3 staining intensities. Since cell density and inter-plate variability can shift the typical bimodal frequency of the histogram, an automatic and adaptive Two-Gaussian curvature-fitting program was developed in Matlab. Cells negative for pSer10-H3 staining are fitted with the first Gaussian curve, and cells positive for pSer10-H3 staining are fitted with the second Gaussian curve. This allows corresponding gate thresholds for positive populations to be adaptively measured according to the Gaussian curvature parameters and reported as a percentage of the cells in each well.

### Statistical analysis of screen data

Statistical analysis was performed using Microsoft Excel. Plate mitotic index values were normalised to the mean of plate medians for each of the DMSO and Monastrol treated data sets. The data was manually curated to remove outliers for each set of 3 replicates. To calculate an average ΔMI for each gene, difference values were calculated by subtracting $MI_{MONA}$- $MI_{DMSO}$ for each of the 3 replicates for each gene. A standard score using the average ΔMI was then calculated for each siRNA. Additionally, the ΔMI was used to perform a two-tailed non-parametric students t-test comparing to a non-targeting siRNA (Qiagen). Genes with a standard score >2 and p-value <0.01 were scored as putative hits for further analysis. As a control for sensitivity of the assay, a siRNA targeting the mitotic kinase Plk1 was used to induce a mitotic arrest and used to calculate a Z-prime score. All plates used in the screen had a Z-prime score >0.5 for Plk1 compared to control siRNA.

### Cell culture and molecular cloning

Cells were grown at 37 °C with 5% $CO_2$. Cal51 and HeLa cells were cultured in DMEM supplemented with 10% FCS and penicillin/streptavidin. RPE cells were cultured in F12:DMEM (1:1) media supplemented with 10% FCS, sodium bicarbonate, Glutamate and penicillin/streptavidin. All transfections were performed as described in the screen except they were performed manually in 96-well or 6-well plates. The sequences of individual siRNA oligos targeting UBE2S are: D2 (ACAAGGAGGUGACGACACU); D4 (CAUGCUGGCGAGCGCGAUA); Q2 (CCGCCUGCUCUUGGAGAACUA); and Q3 (CCCGAUGGCAUCAAGGUCUUU). siRNA targeting CDC20 was a siGENOME smartpool from Dharmacon. Cells were treated with 100 μM Monastrol (Sigma), 50 nM taxol (Sigma), 2.5 μM Dimethylenastron or 5 μM S-trityl-l-cysteine for 20 hours unless otherwise indicated. Cells were synchronised during G1/S-phase of the cell cycle by performing a single thymidine block. A full-length cDNA for human UBE2S was obtained from the Mammalian Gene Collection I.M.A.G.E. consortium (Geneservice). A catalytically inactive version of UBE2S was generated by PCR mutagenesis by making a Ser for Cys substitution at amino acid position 95. Plasmids were verified by restriction enzyme mapping and sequencing.

### Western blotting, immunoprecipitations and antibodies

Western blotting was performed using standard techniques. Primary antibodies were diluted as indicated and incubated with membranes for 2 hours at room temperature: rabbit anti-UBE2S (1:500, Abnova), mouse anti-Cyclin B1 (1:1,000 dilution, Santa Cruz), anti-Securin (1:200, Santa Cruz), anti-Cyclin A (1:500, Santa Cruz), rabbit anti-Nek2A (1:200, BD Bioscience), mouse anti-BUBR1 (1:1,000, a kind gift from Frank McKeon, Harvard Medical School), mouse anti-βactin (1:2,000, Sigma), rabbit anti-CDC20 (1:200, Abcam). HRP-conjugated secondary antibodies were diluted 1:10,000 and incubated with membranes for 1 hour at room temperature, before exposing using ECL. Whole cell extracts for Western

blotting were prepared with ice-cold RIPA buffer (50 mM Tris pH 8.0, 150 mM NaCl, 0.1% SDS, 0.5% sodium deoxycholate, 1% NP40, 0.1% 2-mercapatoethanol, protease inhibitor cocktail (Roche), phosphatase inhibitor cocktail I and II (Sigma)). For co-immunoprecipiatation studies, whole cells extract were prepared with ice-cold NP40 extraction buffer (100 mM Tris pH 7.4, 100 mM NaCl, 0.1% NP40, 0.1% 2-mercapatoethanol, 5 mM EDTA, 10 mM $MgCl_2$, protease inhibitor cocktail (Roche), phosphatase inhibitor cocktail I and II (Sigma)). Extracts were centrifuged at 13,000 rpm for 10 minutes and the soluble fraction collected. CDC20 co-IPs were performed using ~1 μg antibody (sc5296, Santa Cruz) coupled to Protein G sepharose.

### Analysis by flow cytometry

Measurement of DNA content and antibody staining to the mitosis specific marker MPM2 were used to determine the population of mitotic cells. Briefly, ethanol-fixed cells were rinsed with PBS and incubated with mouse anti-MPM2 antibody (1:200 dilution; Upstate) in PBS containing 1% fetal bovine serum (PBS/F) for one hour at 37°C. Cells were washed twice with PBS and incubated with Alexa-488 conjugated goat anti-mouse antibody (1:500 dilution; Invitrogen) in PBS/F for 1 hour at room temperature. Cells were rinsed twice with PBS followed by staining with Propidium Iodide (Sigma) and analyzed using standard methods. Mitotic cells have 4N DNA content and are positive for MPM2 staining.

### Microinjection and time-lapse imaging

For microinjection and microscopy, cells were grown on a Bioptechs ΔT heated stage attached to a Leica DMIRBE microscope or a Zeiss Axiovert 200M microscope equipped with a humidified heated enclosure. Prior to imaging culture medium was replaced with Leibovitz's L-15 medium (Gibco BRL) supplemented with 10% foetal bovine serum and penicillin/streptomycin. Cells were microinjected with 3 ng/μl Cyclin B1-Venus cDNA during G2-phase of the cell cycle using a semiautomatic microinjector (Eppendorf) and assayed by time-lapse DIC and fluorescence microscopy32. EGFP was expressed under an IRES promoter to indentify injected cells. Images were captured at 3 or 5 minutes intervals and analysed by either SlideBook software (Intelligent Imaging Innovations, USA) or Velocity LE Software (Improvision).

### APC/C purification and ubiquitylation assays

HeLa cells were synchronised in G1/S-phase using a single thymidine block for 24 hours followed by a release either in DMA or taxol for 12 hours. Cells were harvested by mitotic shake off, washed in PBS, resuspended in extraction buffer (20 mM HEPES pH 7.8, 175 mM NaCl, 2.5 mM $MgCl_2$, 10% glycerol, 1 mM DTT, 1 mM PMSF, protease inhibitor cocktail (Roche), 2 μM ocadaic acid, 10 nM Microcystin LR, phosphatase inhibitor cocktail II (Calbiochem)). Cells were ruptured using nitrogen cavitation and cleared by centrifugation. APC/C was immunoprecipitated from 10 mg of extract using anti-APC3 antibodies (mAb AF3.1) immobilised to Dynabeads Protein G (Invitrogen). Single reaction were performed at 37°C in 15 μl of QPIP buffer (50 mM PIPES pH 7.5, 100 mM NaCl, 2 mM $MgCl_2$, 10% glycerol, 1 mM DTT, 1 mM EGTA) containing 5 μl of APC3 beads, 300 nM E1, 2.6 μM E2, 150 μM ubiquitin or methyl ubiquitin (Calbiochem), 1 μM BSA, 100 nM CDC20, 100 nM radiolabelled substrate or 10 nM recombinant BUBR1, 2 mM ATP, 2.3 μM creatine kinase and 10 mM creatine phosphate. Reactions were stopped with SDS sample buffer and processed for SDS-PAGE. Dried gels were analysed by a phosphoimager (FLA-5000, FujiFilm) and quantifications were done using MacBas (FujiFilm). BUBR1 ubiquitylation was analysed by Western blotting and subsequent detection by anti-BUBR1 antibodies (Bethyl laboratories). For pre-ubiquitylation experiments Cyclin B1 (1-86) was incubated with APC/C-UBCH10 for 30 minutes and the reaction was stopped by addition of 50 mM DTT. Ubiquitylated Cyclin-B1 species were purified from the reaction mixture by

Strep-Tactin agarose, eluted into QPIP buffer and used as substrates for subsequent in vitro ubiquitylation reactions.

### Protein purification and radiolabelling

E1, His-UBCH10, UBCH5, UBE2S, UBE2S C95S, His-ubiquitin, Cyclin B1-HMK-Strep (amino acid 1-86), Cyclin A-HMK-Strep were expressed in *E.coli*. His-CDC20 and His-BUBR1 were expressed in a baculovirus system. Proteins were purified by Ni-NTA affinity chromatography using standard protocols and the His-tag cleaved by TEV protease as indicated. Cyclin B1 (1-86) and Cyclin A were purified on Strep-tactin beads (IBA, Germany) and radiolabelled with $^{33}$P (Perkin Elmer) by phosphorylation of a C-terminal heart muscle kinase tag (HMK) using protein kinase A (Sigma).

## Supplementary Material

Refer to Web version on PubMed Central for supplementary material.

## Acknowledgments

We thank Dr. Paul Lehner (Cambridge Institute of Medical Research) for providing the ubiquitin-proteasome siRNA library, the Newton Trust (Cambridge) for funding its purchase, and Dr. Lori Passmore for helpful discussions. M.J.G. was supported by a Canadian Institute of Health Research fellowship, J.M., by a FEBS fellowship, and C.G., by a Churchill Foundation Scholarship. M.J.G., C.G. and P.R. were also supported by a UK Medical Research Council (MRC) grant to A.R.V., and J.W., by a Wellcome Trust grant to A.R.V. Work in J.P.'s laboratory is supported by Cancer Research UK, and in A.R.V.'s, by the MRC.

## REFERENCES

1. Musacchio A, Salmon ED. The spindle-assembly checkpoint in space and time. Nat Rev Mol Cell Biol. 2007; 8:379–393. [PubMed: 17426725]
2. Kim SH, Lin DP, Matsumoto S, Kitazono A, Matsumoto T. Fission yeast Slp1: an effector of the Mad2-dependent spindle checkpoint. Science. 1998; 279:1045–1047. [PubMed: 9461438]
3. Nilsson J, Yekezare M, Minshull J, Pines J. The APC/C maintains the spindle assembly checkpoint by targeting Cdc20 for destruction. Nat Cell Biol. 2008; 10:1411–1420. [PubMed: 18997788]
4. Pines J. Mitosis: a matter of getting rid of the right protein at the right time. Trends Cell Biol. 2006; 16:55–63. [PubMed: 16337124]
5. Peters JM. The anaphase promoting complex/cyclosome: a machine designed to destroy. Nat Rev Mol Cell Biol. 2006; 7:644–656. [PubMed: 16896351]
6. Tang Z, et al. APC2 Cullin protein and APC11 RING protein comprise the minimal ubiquitin ligase module of the anaphase-promoting complex. Mol Biol Cell. 2001; 12:3839–3851. [PubMed: 11739784]
7. Aristarkhov A, et al. E2-C, a cyclin-selective ubiquitin carrier protein required for the destruction of mitotic cyclins. Proc Natl Acad Sci U S A. 1996; 93:4294–4299. [PubMed: 8633058]
8. Yu H, King RW, Peters JM, Kirschner MW. Identification of a novel ubiquitin-conjugating enzyme involved in mitotic cyclin degradation. Curr Biol. 1996; 6:455–466. [PubMed: 8723350]
9. Seino H, Kishi T, Nishitani H, Yamao F. Two ubiquitin-conjugating enzymes, UbcP1/Ubc4 and UbcP4/Ubc11, have distinct functions for ubiquitination of mitotic cyclin. Mol Cell Biol. 2003; 23:3497–3505. [PubMed: 12724408]
10. Osaka F, Seino H, Seno T, Yamao F. A ubiquitin-conjugating enzyme in fission yeast that is essential for the onset of anaphase in mitosis. Mol Cell Biol. 1997; 17:3388–3397. [PubMed: 9154838]
11. Rodrigo-Brenni MC, Morgan DO. Sequential E2s drive polyubiquitin chain assembly on APC targets. Cell. 2007; 130:127–139. [PubMed: 17632060]
12. Mathe E, et al. The E2-C vihar is required for the correct spatiotemporal proteolysis of cyclin B and itself undergoes cyclical degradation. Curr Biol. 2004; 14:1723–1733. [PubMed: 15458643]

13. Walker A, Acquaviva C, Matsusaka T, Koop L, Pines J. UbcH10 has a rate-limiting role in G1 phase but might not act in the spindle checkpoint or as part of an autonomous oscillator. J Cell Sci. 2008; 121:2319–2326. [PubMed: 18559889]
14. Rape M, Kirschner MW. Autonomous regulation of the anaphase-promoting complex couples mitosis to S-phase entry. Nature. 2004; 432:588–595. [PubMed: 15558010]
15. Thrower JS, Hoffman L, Rechsteiner M, Pickart CM. Recognition of the polyubiquitin proteolytic signal. EMBO J. 2000; 19:94–102. [PubMed: 10619848]
16. Rieder CL, Maiato H. Stuck in division or passing through: what happens when cells cannot satisfy the spindle assembly checkpoint. Dev Cell. 2004; 7:637–651. [PubMed: 15525526]
17. Gascoigne KE, Taylor SS. Cancer cells display profound intra- and interline variation following prolonged exposure to antimitotic drugs. Cancer Cell. 2008; 14:111–122. [PubMed: 18656424]
18. Brito DA, Rieder CL. Mitotic checkpoint slippage in humans occurs via cyclin B destruction in the presence of an active checkpoint. Curr Biol. 2006; 16:1194–1200. [PubMed: 16782009]
19. Kapoor TM, Mayer TU, Coughlin ML, Mitchison TJ. Probing spindle assembly mechanisms with monastrol, a small molecule inhibitor of the mitotic kinesin, Eg5. J Cell Biol. 2000; 150:975–988. [PubMed: 10973989]
20. Mayer TU, et al. Small molecule inhibitor of mitotic spindle bipolarity identified in a phenotype-based screen. Science. 1999; 286:971–974. [PubMed: 10542155]
21. DeBonis S, et al. In vitro screening for inhibitors of the human mitotic kinesin Eg5 with antimitotic and antitumor activities. Mol Cancer Ther. 2004; 3:1079–1090. [PubMed: 15367702]
22. Gartner M, et al. Development and biological evaluation of potent and specific inhibitors of mitotic Kinesin Eg5. Chembiochem. 2005; 6:1173–1177. [PubMed: 15912555]
23. den Elzen N, Pines J. Cyclin A is destroyed in prometaphase and can delay chromosome alignment and anaphase. J Cell Biol. 2001; 153:121–136. [PubMed: 11285279]
24. Hames RS, Wattam SL, Yamano H, Bacchieri R, Fry AM. APC/C-mediated destruction of the centrosomal kinase Nek2A occurs in early mitosis and depends upon a cyclin A-type D-box. EMBO J. 2001; 20:7117–7127. [PubMed: 11742988]
25. Brito DA, Yang Z, Rieder CL. Microtubules do not promote mitotic slippage when the spindle assembly checkpoint cannot be satisfied. J Cell Biol. 2008; 182:623–629. [PubMed: 18710927]
26. Choi E, et al. BubR1 acetylation at prometaphase is required for modulating APC/C activity and timing of mitosis. EMBO J. 2009
27. Herzog F, et al. Structure of the anaphase-promoting complex/cyclosome interacting with a mitotic checkpoint complex. Science. 2009; 323:1477–1481. [PubMed: 19286556]
28. Ditchfield C, et al. Aurora B couples chromosome alignment with anaphase by targeting BubR1, Mad2, and Cenp-E to kinetochores. J Cell Biol. 2003; 161:267–280. [PubMed: 12719470]
29. Bassermann F, et al. The Cdc14B-Cdh1-Plk1 axis controls the G2 DNA-damage-response checkpoint. Cell. 2008; 134:256–267. [PubMed: 18662541]
30. Stegmeier F, et al. Anaphase initiation is regulated by antagonistic ubiquitination and deubiquitination activities. Nature. 2007; 446:876–881. [PubMed: 17443180]
31. Song L, Rape M. Reverse the curse--the role of deubiquitination in cell cycle control. Curr Opin Cell Biol. 2008; 20:156–163. [PubMed: 18346885]
32. Hagting A, Karlsson C, Clute P, Jackman M, Pines J. MPF localization is controlled by nuclear export. EMBO J. 1998; 17:4127–4138. [PubMed: 9670027]

Europe PMC Funders Author Manuscripts

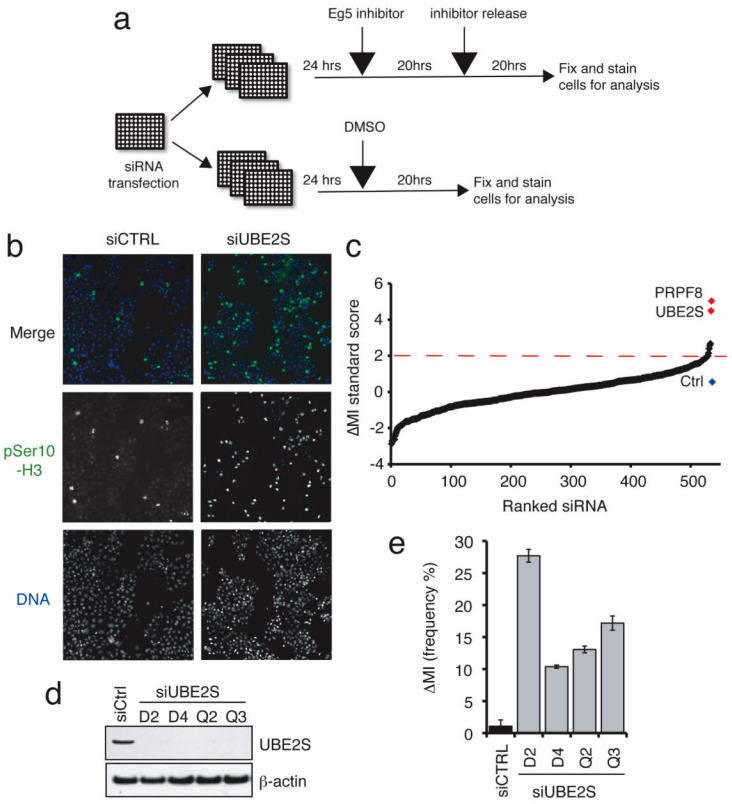


**Figure 1. siRNA screen identifies UBE2S as a modifier of release from arrest at the SAC**

(a) Schematic of screen design using reverse transfection in 96-well plates. (b) Representative fluorescent microscope images from screen data. Cal51 cells were transfected with control or UBE2S siRNA and treated with the Eg5 inhibitor Monastrol as described in (a). Cells are stained for DNA and the mitotic marker phospho-Ser10 Histone H3 (pSer10-H3). DNA staining is used for cell identification. pSer10-H3 staining intensity was measured for >5,000 cells per well and the frequency of pSer10-H3 positive cells reported as a percentage. (c) A graph of ranked ΔMI standard scores (Z-score) for all 535 siRNA included in the screen. The standard score for a non-targeting control siRNA is also presented (coloured blue) and putative hits that give a standard score >2 (dashed red line) and p-value <0.01 are coloured red. (d) Western blots demonstrating efficiency of knockdown using 4 different UBE2S siRNA oligos. β-actin is shown as a loading control. (e) Validation of UBE2S as a screen hit using 4 different siRNA oligos. The ΔMI was determined as described in (a) and in the text.

Europe PMC Funders Author Manuscripts

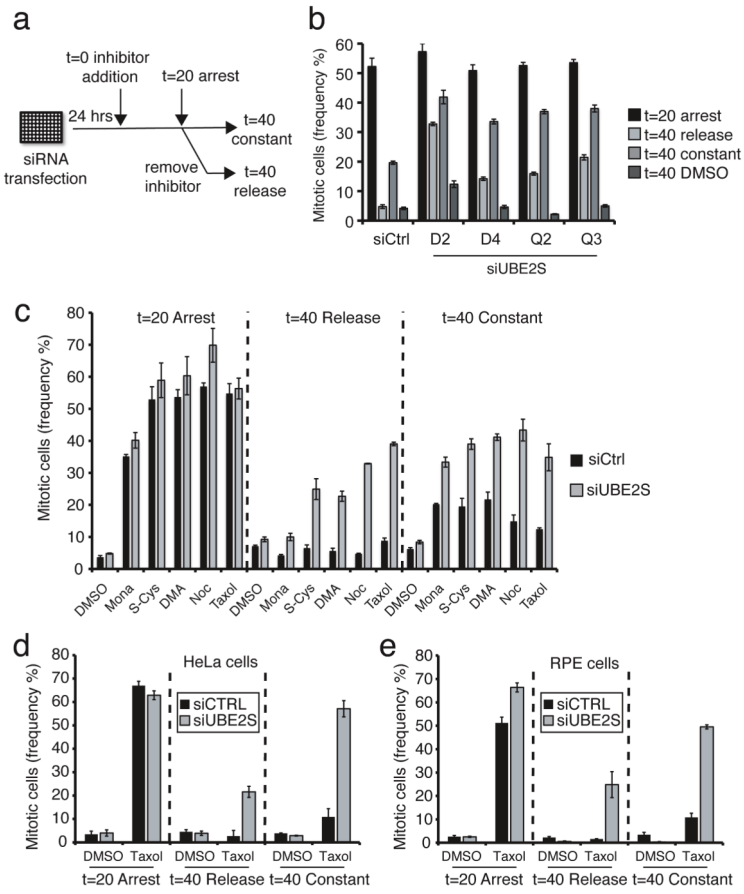


**Figure 2. UBE2S regulates the outcome of drug-induced mitotic arrest**

(a) Schematic of experimental design for a-e. (b) UBE2S prevents release from mitotic arrest. Cells were treated with control or UBE2S siRNA and the mitotic index was measured following arrest with Monastrol. UBE2S-depleted cells were treated with Monastrol for 20 hours (t=20 arrest) and then either released from inhibitor (t=40 release) or left in drug for additional 20 hours (t=40 constant). A DMSO control at t=40 is also shown and the results for 4 different siRNA targeting UBE2S are presented. (c) UBE2S prevents release from mitotic arrest induced by different anti-mitotics. The MI was determined following treatment with DMSO, Monastrol (Mona), S-trityl-l-cysteine (S-Cys), Dimethylenastron (DMA), Nocodazole (Noc) or taxol. (d and e) UBE2S regulates release from mitotic arrest in (d) HeLa and (e) RPE cells. All data are averages of 3 replicates with error bars representing standard deviations.

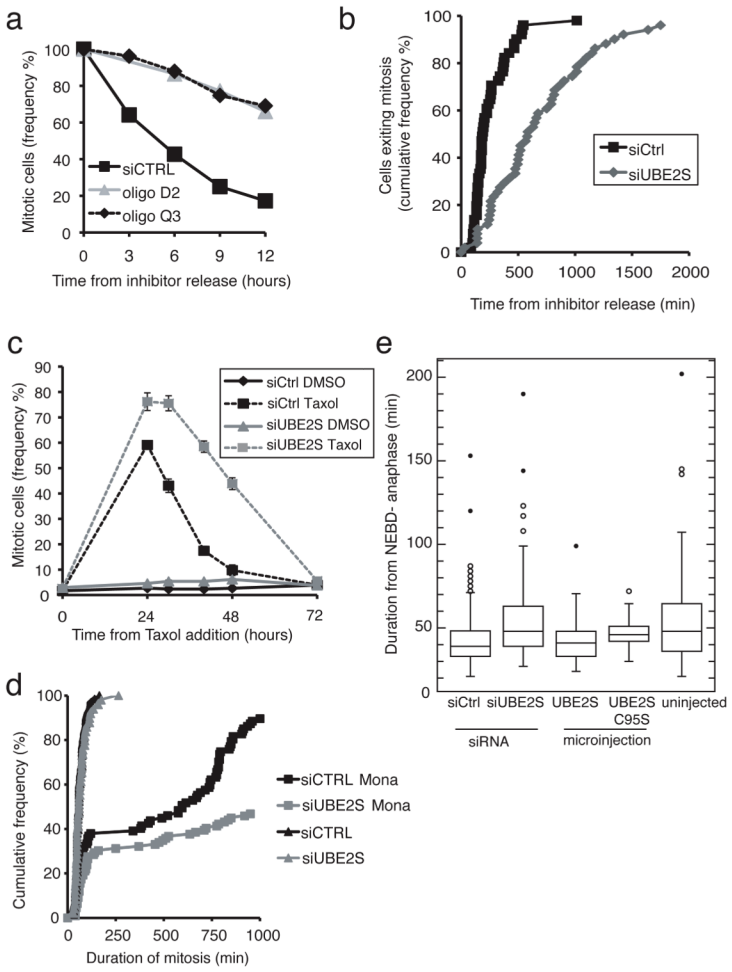


**Figure 3. UBE2S is necessary for mitotic release and slippage**

(a) FACS analysis of cells exiting mitosis following release from arrest. Cells were transfected with control or UBE2S siRNAs (2 different oligos), arrested with Monastrol for 20 hours, collected by mitotic shake-off and analysed following release by FACS staining for the mitotic marker MPM2. (b) Cumulative frequency of cell exiting mitosis determined using DIC time-lapse imaging. Cells were transfected with control or UBE2S siRNA as indicated, arrested for 20 hours before imaging. The time taken to exit mitosis following release was measured based on cellular morphology. (c) A time-course of mitotic index (measured as pSer10-H3 positive cells) following treatment with taxol. Data are the average of 3 replicates with error bars representing standard deviations. Some error bars are too small to be seen. (d) Cumulative frequency graph representing the duration of mitosis following Monastrol treatment as measured by time-lapse imaging. Mitotic arrest induced by Mona is incomplete under the conditions used here, and ~25% of siCTRL and siUBE2S cells complete mitosis within the first ~100 minutes. siUBE2S cells that arrest during mitosis undergo a prolonged arrest compared to siCTRL cells. (e) A box-and-whisker plot showing the duration of an unperturbed mitosis. The duration from NEBD (nuclear envelope breakdown) to anaphase in HeLa cells was measured following depletion of UBE2S (left two plots) or microinjection of cells with a plasmid encoding an untagged version of UBE2S or catalytically inactive UBE2S (C95S). These results are representative of 2 independent experiments.

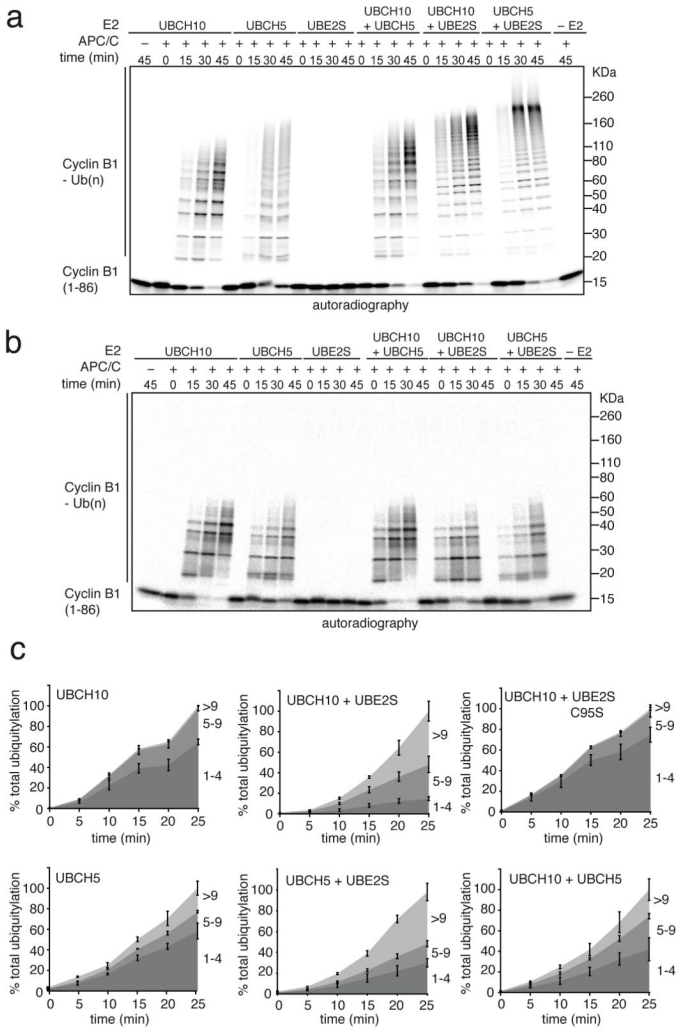


**Figure 4. UBE2S elongates pre-initiated ubiquitin chains on Cyclin B1**

(a) Autoradiograph of an *in vitro* APC/C ubiquitylation assay. Recombinant UBCH10, UBCH5, UBE2S, or the indicated combinations (at 1:1 molar ratio) were used for APC/C *in vitro* activity assays with $^{33}$P-Cyclin B1 (aa1-86) as substrate. Reactions were performed for the indicated time before separation by SDS-PAGE and analysis using a phosphoimager. (b) Same as experiment in (a) but using methyl-ubiquitin to prevent the elongation but not initiation of ubiquitin chains. (c) Quantification of Cyclin B1 ubiquitylation. *In vitro* ubiquitylation reactions were performed as in (a) but with shorter reaction times to prevent limiting amounts of unmodified substrate (Supplemental Information, Fig. S3). Cyclin B1-ubiquitin conjugates with 1-4, 5-9 or >9 ubiquitin molecules (as indicated in Supplemental Information, Fig. S3) from three independent experiments were quantified. Data are normalised to the total amount of ubiquitylated Cyclin B1 and plotted as stacked area charts. Error bars show the SEM.




Europe PMC Funders Author Manuscripts

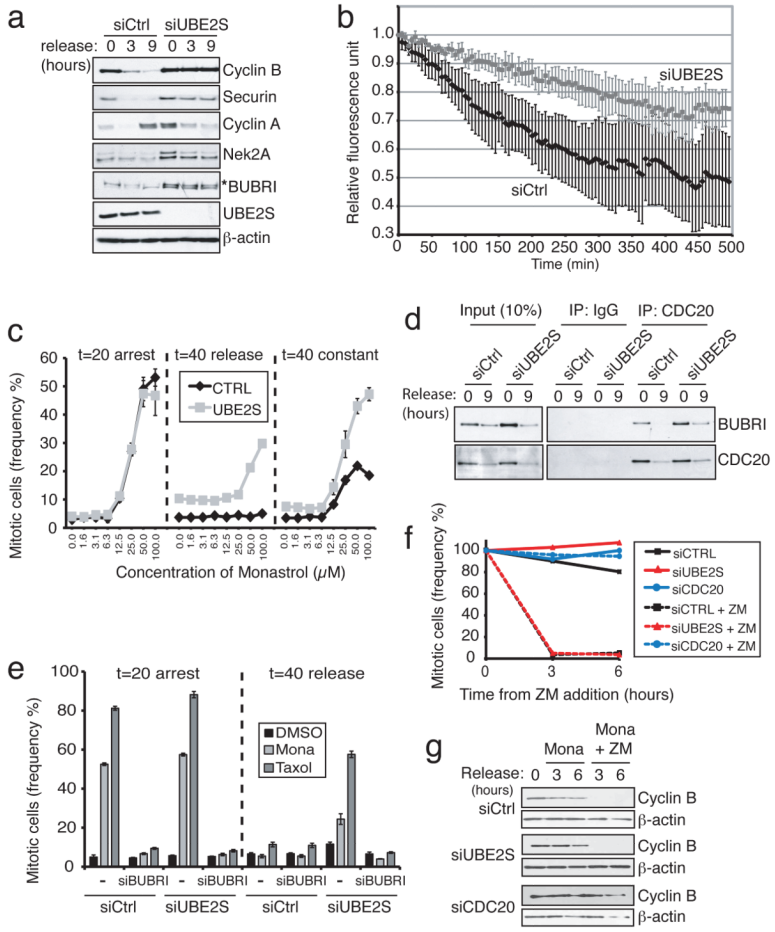


**Figure 5. UBE2S is necessary for degradation of APC/C substrates and to antagonise the SAC**

(a) Western blots for APC substrates following release from a mitotic arrest in control or UBE2S-depleted cells. Cells were arrested for 20 hours in Monastrol, collected by mitotic shake-off, washed 3 times and released into media for 3 and 9 hours. A hyper-phosphorylated form of BUBR1 indicative of checkpoint activation is indicated with an asterisk. Accumulation of Cyclin A is observed 9 hours following release in control cells as cells enter the next cell-cycle. (b) Rate of Cyclin B1 degradation during mitotic arrest. HeLa cells were injected during G2-phase with a plasmid encoding Cyclin B1-Venus and Cyclin B1 degradation analysed by time-lapse fluorescence microscopy in the presence of 100 nM taxol. The fluorescence intensity for each cell is normalised to when Cyclin B1 degradation began. Data are the mean from 6 UBE2S-depleted cells and 14 control cells with error bars representing 95% confidence intervals. These data are representative of 2 independent experiments. (c) Dose-response curve to titration of Monastrol concentrations. Cells were treated with increasing concentrations of Monastrol and the MI determined at t=20 arrest, t=40 release and t=40 constant. Values are the average of 3 replicates and error bars represent standard deviations. In some instances the error bars are too small be seen. (d) Depletion of UBE2S stabilizes SAC activation. The amount of BUBR1 immunoprecipitating with CDC20 was determined. The hyperphosphorylated form of BUBR1 is not observed with the % SDS-PAGE used in this experiment. (e) Inactivation of the SAC bypasses the requirement for UBE2S. The mitotic index in cells co-depleted of UBE2S and BUBR1, and treated with DMSO, Monastrol or taxol. Values are the average of 3 replicates and error bars represent standard deviations. (f and g) Acute inactivation of the checkpoint in arrested cells




Europe PMC Funders Author Manuscripts

overcomes the requirement for UBE2S. Monastrol arrested mitotic cells were treated with the Aurora inhibitor ZM 447439 (ZM) to inactivate the checkpoint and (f) the MI was measured by FACS and (g) Cyclin B1 degradation examined by Western blotting. β-actin blots are shown as a control for loading.



Europe PMC Funders Author Manuscripts